Fluorescence Properties of Pyrimidopyrimidoindole Nucleoside dC^{PPI} Incorporated into Oligodeoxynucleotides

Masahiro Mizuta,[†] Kohji Seio,*[,†,‡] Akihiro Ohkubo,[†,‡] and Mitsuo Sekine*[,†,‡]

CREST, Japan Science and Technology Agency, Department of Life Science, Tokyo Institute of Technology, Nagatsuta, Midoriku, Yokohama 226-8501, Japan

Received: August 25, 2008; Revised Manuscript Received: March 25, 2009

A series of oligodeoxynucleotides labeled by a pyrimidopyrimidoindole deoxynucleoside (**1a**: dC^{PPI}) and its derivatives **2a** and **3a** substituted with electron-donating and -withdrawing groups, respectively, were synthesized according to the phosphoramidite approach. The photophysical properties and quenching efficiencies of oligonucleotides incorporating dC^{PPI} derivatives were studied in detail. The thermal denaturation experiments and molecular dynamics simulation of DNA duplexes incorporating dC^{PPI} suggested that a modified base of dC^{PPI} could form base pairs with guanine and adenine in canonical Watson−Crick and reverse-wobble geometries, respectively. The fluorescence of oligonucleotides incorporating dC^{PPI} derivatives increased upon binding to the counter strands, except when dC^{PPI} and guanine formed a base pair. It was revealed that dGMP quenched the fluorescence of the cyano derivative **3a** most effectively, whereas it affected that of the methoxy derivative **2a** least effectively. The involvement of the electron transfer from guanine to the dC^{PPI} derivatives in the fluorescence quenching was supported by energy considerations.

Introduction

Fluorescent nucleobases that mimic the natural DNA bases have served as sensitive real-time probes of base-stacking and -pairing in their vicinity.[1] These fluorescent nucleosides can be classified into two categories: pyrimidine and purine analogs (Figure 1).

Fluorescent purine analogs, such as 2-aminopurine,[2,3] *etheno*-dA,[4] 3-methylisoxanthopterin,[5] and 6-methylisoxanthopterine[6] have been used for a variety of biological and structural studies of nucleic acids. Several fluorescent pyrimidine analogs have also been reported. For example, pyrrolo-C,[7] 5-furyl-U,[8] benzopyridopyrimidine,[9] and 3,5-diaza-4-oxophenothiazine (tC)[10] have been reported as fluorescent pyrimidine nucleosides that have the capability of Watson−Crick base-pairing.

Recently, we have reported new fluorescent pyrimidine nucleosides, such as a bicyclic 4-*N*-carbamoyldeoxycytidine derivative,[11a] pyrrolopyrimidopyrimidine,[11b] and pyrimidopyrimidoindole nucleoside (dC^{PPI}),[11c,] that have high quantum yields. Among them, dC^{PPI} proved to be the brightest and has the largest Stokes shift of 119 nm. Moreover, dC^{PPI} could be converted to various fluorescent nucleosides that have substituents on the indole ring.

For future fluorescence-based applications of dC^{PPI} and its derivatives, it is very important to clarify their basic properties when they are incorporated into different DNA sequence environments. Considering this, we synthesized a series of oligonucleotides that were labeled with dC^{PPI} or its derivatives substituted with an electron-donating methoxy group or an electron-withdrawing cyano group. Furthermore, we clarified the photophysical properties and quenching efficiencies of these dC^{PPI} derivatives incorporated into oligonucleotides. We also studied the changes in the fluorescence spectra upon duplex formation, the quantum yield (Φ_F) of dC^{PPI} derivatives in both single- and double-stranded DNAs, and the stability and specificity of the duplexes.

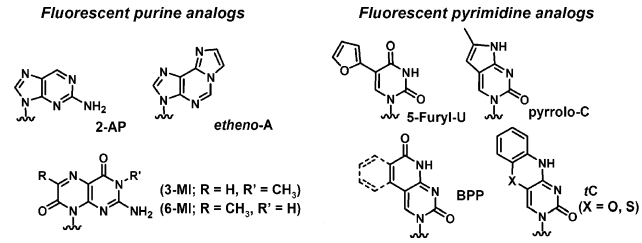

Figure 1. Typical structures of fluorescent purine and pyrimidine analogs.

In this paper, we report details of these studies that will be useful for designing fluorescent oligodeoxynucleotides with dC^{PPI} derivatives to utilize them as new probes for mechanistic clarification of the interaction between nucleic acids and between proteins and nucleic acids.

Results and Discussion

UV-Melting and Molecular Modeling Studies of DNA Duplexes Incorporating dC^{PPI} Derivatives. The dC^{PPI} **1a** and its derivatives **2a** and **3a**, having a methoxy group and a cyano group, respectively, were prepared as described in a previous study.[11c] For the incorporation of the nucleosides **1a**, **2a**, and **3a**, they were converted to the phosphoramidite derivatives **1c**, **2c**, and **3c** by tritylation, followed by the usual phosphitylation, as shown in Scheme 1. We also synthesized the phosphoramidite derivatives of nucleosides **4a** and **5a**, as shown in Scheme S1 of the Supporting Information, which are the 7-*N* and 8-*N* methylated derivatives of **1a**, respectively. Compounds **4a** and **5a** were designed as related derivatives, the structures of which were fixed in the same conjugate systems as two possible tautomeric forms of **1a**.

Using the phosphoramidites, we synthesized oligodeoxynucleotides **OL1**−**OL3** and **OL6**−**OL17**, incorporating **1a**, **2a**,

* Corresponding authors. E-mail: msekine@bio.titech.ac.jp.
† Japan Science and Technology Agency.
‡ Tokyo Institute of Technology.

10.1021/jp807562c CCC: $40.75
Published on Web 06/18/2009

SCHEME 1: Structure of dC^{PPI} (1a), and Its Derivatives 2a, 3a, 4a, and 5a, as well as Their Phosphoramidites

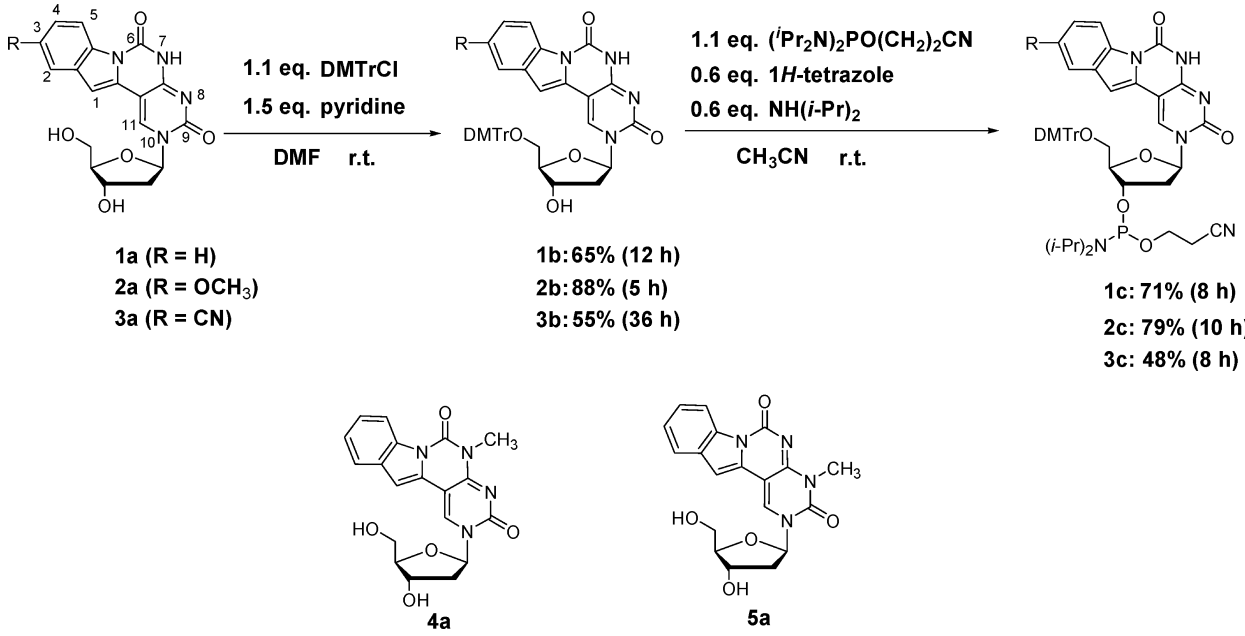

SCHEME 2: Sequences of the Oligodeoxynucleotides Used in This Study

A

5'-d(CGCAATXTAACGC)-3'	5'-d(GCGTTANATTGCG)-3'
OL1: X = **1a**	**c-OL1**: N = G
OL2: X = **2a**	**c-OL2**: N = A
OL3: X = **3a**	**c-OL3**: N = C
OL4: X = C	**c-OL4**: N = T
OL5: X = T	
OL6: X = **4a**	
OL7: X = **5a**	

B

OL8:	5'-d(AATXTATTTATTTAA)-3' /	**c-OL5**:	5'-d(TTAAATAAATAAATT)-3'
OL9:	5'-d(AATXGATTTATTTAA)-3' /	**c-OL6**:	5'-d(TTAAATAAATCAATT)-3'
OL10:	5'-d(AATXTGTTTATTTAA)-3' /	**c-OL7**:	5'-d(TTAAATAAACAAATT)-3'
OL11:	5'-d(AATXTAGTTATTTAA)-3' /	**c-OL8**:	5'-d(TTAAATAACTAAATT)-3'
OL12:	5'-d(AATXTATGTATTTAA)-3' /	**c-OL9**:	5'-d(TTAAATACATAAATT)-3'
OL13:	5'-d(AATXCATTTATTTAA)-3' /	**c-OL10**:	5'-d(TTAAATAAATGAATT)-3'
OL14:	5'-d(AATXTCTTTATTTAA)-3' /	**c-OL11**:	5'-d(TTAAATAAAGAAATT)-3'
OL15:	5'-d(AATXTACTTATTTAA)-3' /	**c-OL12**:	5'-d(TTAAATAAGTAAATT)-3'
OL16:	5'-d(AATXTATCTATTTAA)-3' /	**c-OL13**:	5'-d(TTAAATAGATAAATT)-3'
OL17:	5'-d(GCTTTGTXTCTTTCG)-3' /	**c-OL14**:	5'-d(CGAAAGAAACAAAGC)-3'
	X = **1a**		

3a, **4a**, or **5a** (Scheme 2). We also prepared the complementary strands of these oligodeoxynucleotides, **c-OL1**−**c-OL14**, and studied the fluorescence properties of **1a**, **2a**, and **3a** in DNA duplexes composed of these oligonucleotides.

First, we studied the properties of **OL1**, **OL2**, and **OL3** that have a sequence of 5′-d(CGCAATXTAACGC)-3′, where X represents the nucleoside residues of **1a**, **2a**, and **3a**, respectively, in the presence or absence of the counter strands **c-OL1**, **c-OL2**, **c-OL3**, and **c-OL4** that have 5′-d(GCGTTANATTGCG)-3′ sequences (Scheme 2A). We also synthesized oligodeoxynucleotides **OL4** and **OL5**, incorporating unmodified deoxycytidine and thymidine residues, respectively, and **OL6** and **OL7**, incorporating nucleosides **4a** and **5a**, respectively, at position X for comparison.

We measured the duplex stability of DNA duplexes of **OL1**−**OL5** with the complementary strand **c-OL1** and single-base-mismatched strands, **c-OL2**−**c-OL4**. These results are summarized in Table 1.

We measured the T_m values of the duplexes of **OL1**, in whichthe nucleoside residue at position X was unsubstituted dC^{PPI} (**1a**), and the counter strands **c-OL1**, **c-OL2**, **c-OL3**, and **c-OL4** by changing the nucleoside at position N to G, A, T, or C and compared them with the unmodified duplexes, **OL4/c**−**OL1** and **OL5/c**−**OL2**. When the base at position N was G, the T_m value of the duplex that contained dC^{PPI} (**1a**) was 58 °C, which was almost the same as that of the unmodified double-stranded DNA**OL4/c-OL1** that contained a canonical C−G pair. Moreover, the T_m value of the duplex **OL1/c**−**OL2**, having the A-dC^{PPI} base pair, was 54 °C. This value was lower by only 2.0 °C as compared with that of the **OL5/c**−**OL2** that has the canonical A−T base pair, and this value is much more stable compared with that of the duplex that has an A−C

TABLE 1: Melting Temperatures (°C) of Duplexes Incorporating a dC^{PPI}Derivative[a]

	c-OL1, N = G	c-OL2, N = A	c-OL3, N = C	c-OL4, N = T
OL1 X = **1a**	58	54	48	47
OL2 X = **2a**	55	51	49	47
OL3 X = **3a**	53	51	47	46
OL4 X = C	58	n.t.	n.t.	n.t.
OL5 X = T	n.t.	56	n.t.	n.t.

[a] The T_m values of the duplexes (2 μM) were measured in 50 mM sodium phosphate and 0.1 M sodium chloride (pH 7.0). [b] n.t.: not tested.

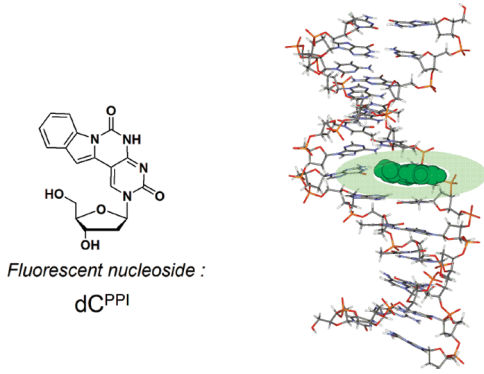

Figure 2. Structure of dC^{PPI} and a DNA duplex modified with dC^{PPI}.

mismatch (data not shown). These results indicated the ability of dC^{PPI} to recognize both guanine and adenine. The same trend was observed in the T_m values of the duplexes formed by **OL2** and **OL3**, in which the nucleoside residue X was **2a** and **3a**, respectively. However, the stabilities of the duplexes formed by **OL2** and **OL3**, having a substituent on the indole rings of dC^{PPI} residues, decreased in comparison to those of the duplexes formed by **OL1** incorporating **1a**, particularly when the dC^{PPI} derivatives formed base pairs with guanine and adenine.

To evaluate the structure of dC^{PPI}-G and dC^{PPI}-A, we performed molecular dynamics (MD) simulations of the duplexes of **OL1/c-OL1** and **OL1/c-OL2**. As shown in Figure 3, the 13-mer double strands were B-type duplexes irrespective of the nucleoside residue at position N, which is indicated by

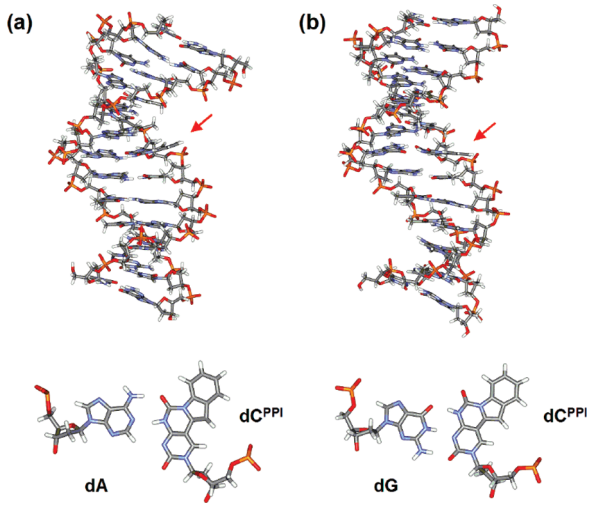

Figure 3. MD simulation of 13-mer duplexes of **OL1** (X = **1a**) and (a) **c-OL2** (N = A) or (b) **c-OL1** (N = G) and the structure of each N-dC^{PPI} pair.

SCHEME 3: Possible Tautomers of 1a

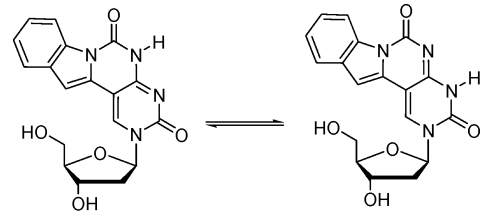

TABLE 2: Photophysical Properties of dC^{PPI} Derivatives Incorporated into Oligonucleotides OL1, OL2, and OL3[a]

	X	N	λ_{max}^{abs}	ε_{366}	λ_{max}^{Flu}	Φ	$\varepsilon_{366} \times \Phi$
OL1	**1a**		383	5822	505	0.030	175
OL1/c-OL1	**1a**	G	390	3957	511	0.015	59
OL1/c-OL2	**1a**	A	385	4718	500	0.062	293
OL1/c-OL3	**1a**	C	379	5708	489	0.106	605
OL1/c-OL4	**1a**	T	385	4718	500	0.052	245
OL2	**2a**		379	7131	503	0.027	193
OL2/c-OL1	**2a**	G	379	5639	508	0.010	56
OL2/c-OL2	**2a**	A	377	5801	499	0.060	348
OL2/c-OL3	**2a**	C	380	7551	492	0.103	778
OL2/c-OL4	**2a**	T	379	6866	496	0.062	426
OL3	**3a**		371	8340	475	0.121	1009
OL3/c-OL1	**3a**	G	378	9449	477	0.019	180
OL3/c-OL2	**3a**	A	378	10270	471	0.108	1109
OL3/c-OL3	**3a**	C	379	9126	465	0.267	2437
OL3/c-OL4	**3a**	T	379	8537	473	0.191	1631

[a] Spectra were measured in 50 mM sodium phosphate and 0.1 M sodium chloride (pH 7.0) at 25 °C.

the arrows. The MD simulation also indicated that the dC^{PPI} residue formed a Watson−Crick base pair with the guanine base and the reverse-wobble base pair with the adenine base. In addition, because the indole region of dC^{PPI} was located in the major groove in the DNA duplexes, the indole ring overlapped with the 5′-upstream thymine, as shown in Figure S1 of the Supporting Information.

In these MD simulations, we assumed that the tautomer form of **1a** was always the 7*H*-form (Scheme 3). This assumption was confirmed by the fact that the absorption maximum of dC^{PPI} in **OL1** was observed at around 378−390 nm, as described in Table 2, whereas that of the tautomer analog of 8-methyl-dC^{PPI} (**5a**) in aqueous solution was 407 nm.[11c]

To obtain further evidence, we measured the fluorescence spectra of **4a** and **5a** in the modified oligonucleotides **OL6** and **OL7** in the single- and double-stranded states (Table S2 of the Supporting Information). The absorption maxima of oligonucleotides incorporating **4a** and **5a** were observed at around 379 and 413 nm, respectively. The absorption maxima were also observed at similar positions in their double-stranded structures formed with **c-OL1**−**c-OL4** (Table S2). Therefore, it was confirmed that tautomerism of the 7*H*-form to 8*H*-form never occurred, even when incorporated into oligonucleotides.

UV Absorption and Fluorescence of dC^{PPI} Derivatives 1a, 2a, and 3a in Oligonucleotides. We characterized the photophysical properties of the dC^{PPI} derivatives incorporated into the above-mentioned oligonucleotides. The absorption and emission spectra of dC^{PPI} derivatives in **OL1**, **OL2**, and **OL3** in their single-stranded states and after hybridization with the counter strand **c-OL1**, **c-OL2**, **c-OL3**, or **c-OL4** were measured in 0.1 M sodium phosphate buffer (pH 7.0), and these data are summarized in Table 2 and shown in the Supporting Information as Figures S2−S8.

The absorption maximum (λ_{max}^{abs}) derived from each dC^{PPI} derivative in **OL1**, **OL2**, or **OL3** was red-shifted by 2−9 nm compared with that of the corresponding nucleoside in an aqueous solution. The red shift of each modified nucleoside was from 374 to 383 nm for **1a**, from 375 to 379 nm for **2a**, and from 369 to 371 nm for **3a**. The red shifts of λ_{max}^{abs} were also observed when **OL1**, **OL2**, or **OL3** was hybridized with the counter strands, **c-OL1**−**c-OL4**. These observations indicated that the dC^{PPI} derivatives stacked between the neighboring nucleobases in both single- and double-stranded states.

Next, we analyzed the maximum fluorescence wavelength, λ_{max}^{Flu}, in the presence and absence of the counter strands. In the single-stranded state, the dC^{PPI} derivatives showed a blue-shifted λ_{max}^{Flu} as compared with those of the nucleosides in an aqueous solution: that is, $\lambda_{max}^{Flu} = 513$ nm[11c] for nucleoside **1a**, 511 nm[11c] for nucleoside **2a**, and 487 nm[11c] for nucleoside **3a**. Similar blue shifts of λ_{max}^{Flu} in comparison with those of nucleosides were also observed in the duplexes incorporating **1a**, **2a**, and **3a**. In particular, it is nothworthy that all three modified oligomers (**OL1**−**OL3**) signal the presence of a C on the opposite strand with the largest blue shift and the most intense emission.

We have recently reported the solvatochromism of dC^{PPI} derivatives, in which their λ_{max}^{Flu} values were blue-shifted when dissolved in less polar methanol compared with that in aqueous solvents. Therefore, the blue shifts of **1a**, **2a**, and **3a** in the single- and double-stranded states could be partially explained by the rather hydrophobic environment in the duplexes.

We also analyzed the λ_{max}^{Flu} value of each duplex in comparison with the corresponding single strand and found interesting shifts of λ_{max}^{Flu} that were dependent on the nucleoside at position N. When dC^{PPI} in **OL-1** was paired with adenine and thymine, its λ_{max}^{Flu} value in the double-stranded state was blue-shifted from 505 to 500 nm in each case. Similarly, **OL2** and **OL3** showed blue shifts from 503 to 499 (for A) and 496 nm (for T) and from 475 to 471 (for A) and 473 (for T) nm, respectively. The blue shifts were more significant when the dC^{PPI} derivatives were paired with cytosine. In contrast, the λ_{max}^{Flu} values were markedly red-shifted to 511 nm in **OL1**, 508 nm in **OL2**, and 477 nm in **OL3** when the dC^{PPI} derivatives were paired with guanine. These results indicated the presence of some photophysical interactions between guanine and dC^{PPI}.

Fluorescence Intensities of dC^{PPI} Derivatives 1a, 2a, and 3a in Oligodeoxynucleotides. The fluorescence intensity and quantum yield (Φ) of dC^{PPI} derivatives **1a** and **2a** in the single- or double-stranded DNA duplexes showed a similar trend. In the single-stranded state, the Φ values of **1a** and **2a** were about 0.03. In the double-stranded state, the Φ values of both **1a** and **2a** were reduced to approximately 0.01 when N was G, increased to 0.05−0.06 when N was A or T, and 0.10 when N was C. These results suggested that the fluorescence of **1a** and **2a** was quenched by the guanine residue.

On the other hand, the Φ values of the dC^{PPI} derivative **3a** in the single- and double-stranded states became larger than the corresponding values of **1a** and **2a** to give ∼0.1 for N = A, 0.19 for N = T, and 0.27 for N = C. When the opposite base was a guanine residue, the dC^{PPI} derivative **3a** was quenched to a level of 0.019, which is observed in the case of **1a** and **2a**.

These results suggested that the Φ values of the double-stranded states, having cytosine at position N, increased significantly by 2−3-fold compared with those of the single-stranded state in all modified oligonucleotides. We also calculated a more practical parameter (i.e., brightness) by multiplying ε_{366} and Φ values. Except for the cases of N = G, the brightness of all of the dC^{PPI} derivatives in the double-stranded state was greater compared with that in the single-stranded state. The quenching of fluorescence molecules by the surrounding guanine residues is well-known in the literature. The mechanism of the quenching is believed to involve an electron transfer from a guanine residue to an excited fluorophore because of the lower oxidation potential of guanine.[12−15] Interestingly, Okamoto and co-workers suggested that the electron transfer efficiency from guanine to fluorescent nucleobases could be enhanced by hydrogen bond formation between the nucleobases.[9a] Therefore, we checked the effect of hydrogen-bond formation between **1a** and guanine on fluorescence quenching. and we measured the fluorescence properties of **OL6**, in which the nucleoside residue at position X was replaced by the tautomer analog **4a** in the single- and double-stranded states with **c-OL1** to **c-OL4** and compared them with the fluorescence properties of **OL1**. The results for **OL6** are shown in Table S2.

As a result, the ratio of the Φ value of **OL1/c-OL1** to that of the single-stranded **OL1** was 0.5. Similarly, the Φ values of **OL2/c-OL1** and **OL3/c-OL1** duplexes to the corresponding single strands were determined to be 0.37 and 0.16, respectively. In contrast, the ratio of **OL6/c-OL1** duplexes, which contained the tautomer analog **4a**, increased significantly to 0.87, probably because of the presence of the methyl group at the hydrogen bond site. This result suggested that electron transfer from the guanine residue to the dC^{PPI} derivatives occurred more efficiently, when hydrogen bonds were formed between the dC^{PPI} derivatives and the guanine residue.

Quenching Properties of dC^{PPI} Derivatives in Aqueous Solution. As described above, the fluorescence of dC^{PPI} derivatives was quenched by the guanine residue. To further evaluate the quenching of dC^{PPI} derivatives by guanine, steady-state fluorescence quenching was analyzed at the nucleoside level using the Stern−Volmer equation[16] (eq 1), where F and F_0 are the fluorescence intensities in the presence and absence of a quencher Q (dGMP) and K_{sv} is a quenching constant.

$$F_0/F = 1 + K_{sv}[Q] \quad (1)$$

These results are shown in the Supporting Information as Figure S9, and the numerical data as the free nucleosides and that in the presence of 50 mM GTP are shown in Table 4. As shown in the column that indicates λ_{max}^{abs} values, the absorption maxima of all dC^{PPI} derivatives showed bathochromic shifts of 1−7 nm upon addition of 50 mM dGMP. The red shifts of the absorption maxima indicated the formation of some complexes between the dC^{PPI} derivatives and dGMP.

The plots of the F_0/F values against the dGMP concentrations resulted in linear graphs (Figure S9). Each K_{sv} value was obtained from the slope of the line and is listed in Table 3. Among **1a**, **2a**, and **3a**, compound **2a** with the methoxy group

TABLE 3: Spectroscopic Characterization and Quenching Constants of dC^{PPI}Derivatives with dGMP[a]

compd	λ_{max}^{abs} (nm)	λ_{max}^{Flu} (nm)	K_{sv} (M^{-1})
1a	374	513	
1a + dGMP	381	512	15.2
2a	375	511	
2a + dGMP	381	511	5.5
3a	369	487	
3a + dGMP	370	485	62.8

[a] Fluorescence spectra were measured in 50 mM phosphate buffer containing 0.1 M sodium chloride at pH 7.4 in the presence or absence of 50 mM dGMP.

TABLE 4: Electron Transfer Free Energies of dC^{PPI} Derivatives in Aqueous Solution[a]

	E_{ox} (V)	E_{red} (V)	$E_{0,0}$ (eV)	ΔG_{et} (eV)
1a	0.89	−1.41	2.87	−0.37
2a	0.90	−1.42	2.87	−0.36
3a	1.03	−1.39	2.96	−0.48

[a] Redox potentials were measured in 50 mM phosphate buffer containing 10% DMSO (v/v) and 0.1 M sodium chloride, pH 7.4. E_{ox} and E_{red} are the observed values vs Ag/AgCl. ΔG_{et} (vs SHE) was calculated by considering the correction in difference (0.199 V) between Ag/AgCl and SHE.

showed the smallest K_{sv} value of 5.5, which suggested suppression of fluorescent quenching by the methoxy group. On the other hand, **3a** had the largest K_{sv} value, which suggested the most efficient quenching by dGMP.

Next, we studied the electron transfer from guanine to dC^{PPI} derivatives energetically. Photoinduced electron transfer (PET) from guanine to excited rhodamine,[12] oxazine,[13] or stilbene dyes[14] is a well-known process. Similar insights into distance-dependent electron transfer kinetics in DNA have been provided by V. Shafirovich et al. using 2-aminopurine as a probe.[3] The fact that the photoexcited dC^{PPI} derivatives were quenched more by guanine than by cytosine, thymine, and adenine, as shown in Table 2, was consistent with the PET mechanism,[15] in which the excited dC^{PPI} derivatives served as the electron acceptors, and the guanine base, as a ground-state electron donor. Progress of the PET reactions is determined by the free energies of the reactions, the reorganization energies, and the distances between the donors and acceptors.

First, to investigate the photoinduced electron transfer efficiency between **1a**, **2a**, or **3a** and guanine, the free-energy change for the electron transfer ΔG_{et} was estimated using the Rehm−Weller equation[17] (eq 2), where C is the solvent-dependent Coulombic attraction energy, which can be neglected in polar solvents such as water, and the E_{ox} of guanosine is 1.29 V (vs NHE) at pH 7.[18]

$$\Delta G_{et} = (E_{ox} \text{ of guanosine}) - (E_{red} \text{ of } \mathbf{1a}, \mathbf{2a}, \text{ or } \mathbf{3a}) - (E_{0,0} \text{ of } \mathbf{1a}, \mathbf{2a}, \text{or } \mathbf{3a}) + C \quad (2)$$

The E_{red} values of **1a**, **2a**, and **3a** were measured using cyclic voltammetry as shown in Figure S10 of the Supporting Information. Table 4 shows the one-electron redox potentials (vs Ag/AgCl) and the corresponding transition energy, $E_{0,0}$, of dC^{PPI} derivatives. The $E_{0,0}$ value was calculated using $E_{0,0} = (E^{abs}_{max} + E^{Flu}_{max})/2$ to be ∼2.9 eV for the dC^{PPI} derivatives. ΔG_{et} from the ground-state guanine to the excited dC^{PPI} derivatives can be estimated as approximately −0.36 to −0.48 eV.

These data demonstrated that the electron transfer reaction between dC^{PPI} derivatives and guanine was exergonic. The observation that the fluorescence of dC^{PPI} derivatives was efficiently quenched by the dC^{PPI}/dG base pair in oligonucleotides was consistent with the negative signs of the ΔG_{et} values.

Distance Dependence of Fluorescence Quenching between dC^{PPI} (1a) and Guanine in Modified Oligonucleotides. The above-mentioned experiments revealed that the fluorescence of the dC^{PPI} derivatives could be quenched by contact with the guanine residue of the duplexes in aqueous solutions. We next studied the quenching of the fluorescence of **1a** by the guanine residues remote from **1a** (Table 5).

We studied the quenching of **1a** by a guanine residue when it existed in the same strand (**OL9**−**OL12**) and in the complementary strand (**c-OL10**−**c-OL13**), as shown in Scheme 2B. In these cases, adenine was chosen as the base to be paired with **1a** to avoid the electron transfer between the paired bases.

TABLE 5: Distance Dependence of the Quenching between dC^{PPI}(1a) and the Guanine Base[a]

	sequence	Φ
OL8/c-OL5	5′-AAT**X**TATTTATTTAA-3′ 3′-TTAAATAAATAAATT-5′	0.059
OL9/c-OL6	5′-AAT**X**G**A**TTTATTTAA-3′ 3′-TTAACTAAATAAATT-5′	0.030
OL10/c-OL7	5′-AAT**X**T**G**TTTATTTAA-3′ 3′-TTAAACAAATAAATT-5′	0.057
OL11/c-OL8	5′-AAT**X**TA**G**TTATTTAA-3′ 3′-TTAAATCAATAAATT-5′	0.057
OL12/c-OL9	5′-AAT**X**TAT**G**TATTTAA-3′ 3′-TTAAATACATAAATT-5′	0.055
OL13/c-OL10	5′-AAT**X**CATTTATTTAA-3′ 3′-TTAA**G**TAAATAAATT-5′	0.048
OL14/c-OL11	5′-AAT**X**TCTTTATTTAA-3′ 3′-TTAAA**G**AAATAAATT-5′	0.051
OL15/c-OL12	5′-AAT**X**TACTTATTTAA-3′ 3′-TTAAAT**G**AATAAATT-5′	0.050
OL16/c-OL13	5′-AAT**X**TATCTATTTAA-3′ 3′-TTAAATA**G**ATAAATT-5′	0.054

[a] Spectra were measured in 50 mM sodium phosphate and 0.25 M sodium chloride (pH 7.0) at 10 °C. The dC^{PPI} residue is denoted by **X**.

TABLE 6: Quantum Yields of Oligonucleotides Incorporating dC^{PPI} (X = 1a)[a]

	sequence	Φ
OL17	5′-GCTTTGT**X**TCTTTCG-3′	0.005
OL17/c-OL14	5′-**G**CTTT**G**T**X**TCTTTC**G**-3′ 3′-C**G** AAACAAA**G**AAA**G**C-5′	0.041

[a] Spectra were measured in 50 mM sodium phosphate and 0.25 M sodium chloride (pH 7.0) at 10 °C. The dC^{PPI} residue is denoted by **X**.

These results are shown in Table 5. The dC^{PPI} residue in the **OL8/c-OL5** duplex showed a Φ value of 0.059. When the nucleoside residue adjacent to the 3′-side of the dC^{PPI} was changed to guanine, as in the case of the **OL9/c-OL6** duplex, the fluorescence was efficiently quenched to give a Φ value of 0.030, which corresponded to a 51% reduction to that of **OL8/c-OL5**. However, the fluorescence recovered to give a Φ value of 0.057 by separation of the guanine residue and dC^{PPI} by only a single nucleoside residue, as in the case of **OL10/c-OL7.** The fluorescence intensities were essentially unchanged by further separation of these residues, as shown in the case of **OL11/c-OL8** and **OL12/c-OL9** duplexes. These results clearly indicated that electron transfer occurred efficiently only when the guanine and dC^{PPI} residues were in contact with each other in a stacking geometry.

Next, we studied the electron transfer between **1a** and G when they were in the opposite strands using **OL13** to **OL16** with their complementary strands. In the case of the **OL13/c-OL10** duplex, which contains guanine at the position next to the adenine residue paired with dC^{PPI}, the Φ value was smaller compared with that of **OL8/c-OL5**, but larger compared with that of **OL9/c-OL6** containing the guanine base stacked with the dC^{PPI}. Therefore, fluorescence quenching of dC^{PPI} by the unstacked guanine proved to be less effective. The interstrand quenching was suppressed to the level of Φ = 0.051−0.054 by separating **1a** and the guanine residue, as shown by the Φ values of **OL14/c-OL11**, **OL15/c-OL12**, and **OL16/c-OL13**.

The emission spectra of the above-mentioned duplexes are shown in Figure S11A−C of the Supporting Information.

The quenching experiments provided useful information for designing fluorescent oligodeoxynucleotides (ODNs) incorporating dC^{PPI} and multiple guanine residues. To keep the fluorescence strong, the guanine residues and dC^{PPI} incorporated into the same strand should be separated by at least a nucleotide residue, and the guanine residue can be incorporated into any position of the opposite strands other than the base-pairing site, because the quenching from the guanine residue in the opposite strand was small, as indicated by comparison of **OL8/c-OL5** and **OL13/c-OL10**. Such expectation was confirmed by the synthesis of the **OL17/c-OL14** duplex containing a dC^{PPI} residue and six guanine residues, as shown in Figure S11D. A single-stranded oligomer, **OL17**, showed only weak fluorescence of $\Phi = 0.005$ because the conformational flexibility of the single strand enabled the dC^{PPI} to contact with the surrounding aqueous media and the guanine residues in the same strand (Table 6). However, upon duplex formation with **c-OL14**, the quantum yield of the duplex **OL17/c-OL14** increased to 0.041, which is a value comparable to those of the duplexes that contain a single guanine residue. These results indicated that the DNA duplexes incorporating **1a** can retain a rather large fluorescence signal, even in the presence of many guanine residues, so long as they form duplex structures and the distances from the guanine residues are appropriately designed.

Conclusion

In this paper, we described the photochemical properties of oligonucleotides fluorescent-labeled with dC^{PPI} **1a** and its derivatives **1b** and **1c**. The fluorescence of oligonucleotides incorporating dC^{PPI} derivatives was quenched upon the base pairing with the guanine residue in the counter strand, probably due to the electron transfer mechanism. Such property might be useful for the detection of the guanine residue in the counterstrand when these modified nucleosides were applied to the SNPs analyses and the gene detection. In addition, the fluorescence was also quenched by the guanine residue in the own strand. This intrastrand quenching could be effectively used to suppress the fluorescence of **1a** in the single strand state. As we also demonstrated in Table 6, the florescence quantum yield of the duplex state could be increased by 8 times in comparison to that of the single strand state by the appropriate design of the positions and the numbers of the guanine residue (Table 6). These fluorescent properties of the dC^{PPI} derivatives are possibly useful for the development of hybridization-dependent fluorescent probes for gene detection and structural study of nucleic acids. The development of nucleic acid analysis systems, such as DNA microarray and PCR systems, utilizing the dC^{PPI} are on due course in our laboratory and will be reported elsewhere.

Experimental Section

General Methods. ^{1}H, ^{13}C, and ^{31}P NMR spectra were recorded at 500, 125, and 202 MHz, respectively. The chemical shifts were measured from tetramethylsilane (0 ppm) or DMSO-d_6 (2.49 ppm) for ^{1}H NMR or $CDCl_3$ (77.0 ppm) or DMSO-d_6 (39.7 ppm) for ^{13}C NMR.

3-Methoxy-10-[2-deoxy-5-*O*-(4,4′-dimethoxytrityl)-β-D-ribofuranosyl]pyrimido[4′,5′:4,5]pyrimido[1,6-*a*]indole-6,9(7*H*)-dione (2b). To a stirred solution of **1b** (0.77 mmol, 305 mg) and pyridine (1.2 mmol, 93 μL) in DMF (11 mL) was added dimethoxytrityl chloride (0.8 mmol, 272 mg) at room temperature. After 5 h, the reaction mixture was diluted with water and extracted with chloroform. The combined organic layers were washed with saturated $NaHCO_3$ solution, water, and brine; dried over $MgSO_4$; and concentrated under reduced pressure. The crude product was purified by C-200 silica gel chromatography with $CHCl_3$−MeOH−0.5% Et_3N to give **2b** (474 mg, 88%): ^{1}H NMR (DMSO-d_6) δ 2.29−2.35 (2H, m), 3.02−3.07 (1H, m), 3.22−3.25 (1H, dd, $J = 4.8$, 10.6 Hz), 3.56−3.58 (1H, dd, $J = 2.9$, 10.5 Hz), 3.67 (3H, s), 3.68 (3H, s), 3.82 (3H, s), 4.38−4.40 (1H, dd, $J = 3.3$, 7.4 Hz), 4.54−4.56 (1H, m), 5.78 (1H, s), 6.44 (1H, t, $J = 6.4$ Hz), 6.68 (1H, d, $J = 2.5$ Hz), 6.76−6.81 (4H, m), 6.83−6.85 (1H, dd, $J = 2.5$, 9.3 Hz), 7.18 (1H, t, $J = 7.3$ Hz), 7.19−7.27 (3H, m), 7.30−7.32 (4H, m), 7.43−7.45 (9H, m), 8.21 (1H, d, $J = 2.5$ Hz), 8.74 (1H, s). ^{13}C NMR (DMSO-d_6) δ 42.3, 55.2, 55.5, 63.5, 71.9, 86.9, 87.1, 88.5, 97.0, 99.4, 102.8, 112.9, 113.4, 116.2, 127.2, 128.1, 128.4, 128.7, 129.9, 130.0, 130.8, 135.5, 135.7, 138.4, 144.3, 146.3, 154.2, 156.8, 157.3, 158.7. ESI-MS *m*/*z* calcd for $C_{40}H_{36}N_4NaO_8$ [M + Na] 723.2431; found 723.2462.

3-Cyano-10-[2-deoxy-5-*O*-(4,4′-dimethoxytrityl)-β-D-ribofuranosyl]pyrimido[4′,5′:4,5]pyrimido[1,6-*a*]indole-6,9(7*H*)-dione (3b). In a manner similar to that described for the synthesis of **2b**, **3a** (0.076 mmol, 30 mg) was treated with pyridine (0.114 mmol, 9 μL) and dimethoxytrityl chloride (0.084 mmol, 28.4 mg) to give **3b** (29 mg, 55%): ^{1}H NMR (DMSO-d_6) δ 2.38 (1H, m), 3.11 (1H, m), 3.24−3.25 (1H, m), 3.62−3.63 (1H, m), 3.70 (6H, s), 4.37 (1H, s), 4.61 (1H, s), 5.75 (1H, s), 6.48 (1H, s), 6.80−6.85 (4H, m), 7.18−7.48 (9H, m), 8.18 (1H, s), 8.91 (1H, s). ^{13}C NMR (DMSO-d_6) δ 42.6, 55.5, 63.6, 72.1, 87.2, 87.5, 88.9, 96.7, 98.8, 107.6, 113.7, 116.3, 119.5, 125.1, 127.0, 127.6, 128.4, 128.4, 129.9, 130.1, 130.3, 130.6, 135.4, 135.6, 135.8, 140.2, 144.4, 146.4, 146.6, 154.4, 157.8, 158.9. ESI-MS *m*/*z* calcd for $C_{40}H_{33}N_5NaO_7$ [M + Na] 718.2278; found 718.2290.

3-Methoxy-10-[2-deoxy-5-*O*-(4,4′-dimethoxytrityl)-β-D-ribofuranosyl]pyrimido[4′,5′:4,5]pyrimido[1,6-*a*]indole-6,9(7*H*)-dione 3′-(2-cyanoethyl *N*,*N*′-diisopropylphosphoramidite) (2c). Coumpound **2b** was taken up in anhydrous acetonitrile, and the solvent was removed under reduced pressure (×5). To a stirred solution of **2b** (0.47 mmol, 330 mg), diisopropylamine (0.28 mmol, 29 mg), and 1-*H* tetrazole (0.28 mmol, 20 mg) in anhydrous dichloromethane (5 mL) was added 2-cyanoethyltetraisopropylphosphoramidite (0.52 mmol, 156 mg). The solution was stirred at room temperature under argon for 1 h. The reaction was diluted with water, and extracted with chloroform. The combined organic layers were washed with 0.1 N NaOH aq. (×2), water, and brine; dried over $MgSO_4$; and concentrated under reduced pressure. The crude product was purified by C-200 silica gel chromatography with $CHCl_3$−MeOH−0.5% Et_3N to give **2c** (336 mg, 79%). ^{1}H NMR ($CDCl_3$) δ 1.08 (3H, d, $J = 6.8$ Hz), 1.18 (9H, d, $J = 6.6$ Hz), 2.39−2.46 (2H, m), 2.64 (1H, t, $J = 6.1$ Hz), 2.86−2.99 (1H, m), 3.29−3.35 (1H, m), 3.55−3.79 (11H, m), 3.85 (3H, s), 4.36−4.38 (1H, m), 4.64−4.65 (1H, m), 5.69 (1H, s), 6.38−6.43 (1H, m), 6.64−6.67 (1H, m), 6.82−6.85 (4H, m), 6.90 (1H, s), 7.22−7.50 (9H, m), 8.31−8.33 (1H, m), 8.77 (1H, s). ^{13}C NMR ($CDCl_3$) δ 20.5 (m), 24.8 (m), 41.1 (d), 41.4 (d), 43.2 (m), 55.1, 55.5, 58.1 (m), 62.5 (d), 72.1 (d), 72.8 (d), 85.9 (d), 86.1 (d), 86.7, 87.8, 96.7 (d), 99.3 (d), 102.8 (d), 112.7, 113.3, 116.3, 117.4 (d), 127.2 (d), 128.0, 128.1, 128.2, 128.4 (d), 128.6 (d), 129.9 (m), 130.7, 135.2 (d), 135.5, 138.4 (d), 144.0, 146.1, 153.5 (d), 156.7, 157.3, 158.6; ^{31}PNMR ($CDCl_3$) δ 149.9, 150.5. ESI-MS *m*/*z* calcd for $C_{49}H_{53}N_6NaO_9P$ [M + Na] 923.3509; found 923.4293.

3-Cyano-10-[2-deoxy-5-*O*-(4,4′-dimethoxytrityl)-β-D-ribofuranosyl]pyrimido[4′,5′:4,5]pyrimido[1,6-a]indole-6,9(7H)-dione 3′-(2-cyanoethyl *N*,*N*′-diisopropylphosphoramidite)

(3c). In a manner similar to that described for the synthesis of **2c**, **3b** (0.14 mmol, 95 mg) was treated with diisopropylamine (0.08 mmol, 12 μL), 1*H*-tetrazole (0.08 mmol, 6 mg) and 2-cyanoethyltetraisopropylphosphoramidite (0.15 mmol, 45 mg) to give **3c** (59 mg, 48%): ^{1}HNMR ($CDCl_3$) δ 1.03−1.04 (3H, m), 1.14−1.15 (9H, m), 2.42 (1H, t, J = 6.2 Hz), 2.48−2.64 (2H, m), 2.82−2.92 (1H, m), 3.29−3.35 (1H, m), 3.51−3.87 (11H, m), 4.29−4.34 (1H, m), 4.68−4.71 (1H, m), 5.61 (1H, s), 6.38−6.42 (1H, m), 6.68−6.84 (4H, m), 7.18−7.53 (11H, m), 8.55 (1H, s), 8.97 (1H, s); ^{13}C NMR ($CDCl_3$) δ 20.3 (m), 24.5 (m), 40.9 (d), 41.4 (d), 43.2 (m), 55.1 (m), 57.9 (d), 58.1 (d), 62.0 (d), 71.5 (d), 71.9 (d), 85.8 (d), 86.1 (d), 86.8 (d), 87.8 (d), 96.0, 98.8 (d), 107.5 (d), 113.3, 116.5 (d), 117.4 (d), 119.4 (d), 125.0 (d), 126.9 (d), 127.4 (d), 128.2 (m), 129.9 (m), 130.1 (d), 130.3 (d), 135.1 (d), 135.4 (m), 140.1 (d), 144.0 (d), 146.1 (d), 153.4 (d), 157.3 (d), 158.8 (m). ^{13}P NMR ($CDCl_3$) δ 150.2, 150.6. ESI-MS *m*/*z* calcd for $C_{49}H_{51}N_7O_8P$ [M + H] 896.3537; found 896.3574.

Oligonucleotide Synthesis and Characterization. Oligodeoxynucleotides were synthesized according to the conventional phosphoramidite method using a commercially available synthesizer. Oligonucleotides were purified by reversed-phase liquid chromatography on a C18 column, eluting with a gradient of acetonitrile in 0.1 M ammonium acetate buffer. The purity and concentration of the synthesized ODNs containing modified nucleotides were determined by complete digestion with calf intestine alkaline phosphatase (50 U/mL), snake venom phosphodiesterase (11 μg), and P1 nuclease (0.3 U/μL) to 2′-deoxymononucleosides at 37 °C for 6 h.

Hyperchromicities and Extinction Coefficients of the ODNs. Each ODN (0.25 OD units at 260 nm) was enzymatically hydrolyzed under the conditions described above. The hyperchromicity of each ODN was determined by comparing the UV absorbances at 260 nm of its solutions before and after hydrolyses. The extinction coefficient (at 260 nm) of each ODN was determined using the following equation: ε_{ODN} = the sum of $\varepsilon_{nucleoside}$/hyperchromicity. The extinction coefficients (at 260 nm) of the natural nucleosides used for calculations were as follows: d*A*, 15 340; d*C*, 7600; d*G*, 12 160; *T*, 8700. The extinction coefficients for the nucleosides at 260 nm were determined to be the following: dC^{PPI}, 11 000.

Thermal Denaturation Experiments. UV melting experiments were conducted using a UV spectrometer equipped with a temperature controller. All measurements were conducted in a buffer containing 0.1 or 0.25 M NaCl and 50 mM phosphate buffer at pH 7.0. Oligonucleotides were mixed in 1:1 stoichiometry with 2.0 μM single-strand oligonucleotide concentration. Melting curves were recorded at 260 nm in a consecutive heating−cooling−heating cycle (10−90 °C) with a temperature gradient of 0.5 °C/min.

Fluorescence Experiments. Fluorescence spectra were obtained at 10 or 25 °C in a 1-cm path-length cell. The fluorescence quantum yield (Φ) was determined using 0.1 M quinine as reference with a known Φ value of 0.53 in H_2SO_4.[19] The quantum yield was calculated according to the following equation:

$$\frac{\Phi_{F(S)}}{\Phi_{F(R)}} = \frac{A_{(S)}}{A_{(R)}} \times \frac{(Abs)_{(R)}}{(Abs)_{(S)}} \times \frac{{n_{(S)}}^2}{{n_{(R)}}^2}$$

Here, $\Phi_{F(S)}$ and $\Phi_{F(R)}$ are the fluorescence quantum yields of the sample and reference, respectively; $(Abs)_{(S)}$ and $(Abs)_{(R)}$ are the respective optical densities of the sample and reference solution at the wavelength of excitation, and $n_{(S)}$ and $n_{(R)}$ are the values of the refractive index for the respective solvents. Sample excitation was performed with λ_{ex} = 366 nm.

Electrochemical Measurement. Cyclic voltammetry (CV) was measured using an electrochemical analyzer with a single compartment cell equipped with a Pt working electrode, Pt counter electrode, and a reference electrode (Ag/AgCl).

Molecular Dynamics Simulation. Force field parameters were taken from the Cornell et al.[20] force field. Partial charges were calculated following the RESP protocol based on quantum chemical calculations at the HF/6-31G(d) level using Gaussian 03.[21] All MD simulations were performed with the Sander module of the Amber 8 package in a periodic box, including explicit TIP3 water molecules and the parm94 force field. Initial positions of additional sodium ions were determined using the xleap module of the Amber package. The conformations of the solvated triplexes were first relaxed via energy minimization. Following minimization, the systems were gradually heated from 0 to 300 K with positional restraints over a period of 0.05 ns. During another 0.35 ns simulation time at 300 K, the positional restraining force constant was gradually reduced from 10 kcal mol^{-1} to zero. Each simulation was continued for a total simulation time of 3.4 ns.

Acknowledgment. This work was supported by a grant-in-aid from CREST (JST) and Industrial Technology Research Grant Program in 2005 of the New Energy and Industrial Technology Development Organization (NEDO) of Japan. This study was also supported by a KAKENHI 20350074 and in part by a grant of the Genome Network Project from the Ministry of Education, Culture, Sports, Science and Technology, Japan.

Supporting Information Available: Spectroscpic and cyclic voltammograms of the oligonucleotides and nucleosides. Synthesis of dC^{PPI} derivatives, m^7H (**4a**) and m^8H (**5a**) building blocks, and the photophysical properties of modified oligonucleotides containing m^7H (**4a**) and m^8H (**5a**). MALDI-TOF-MS data of dC^{PPI} derivative-containing oligonucleotides. Quenching titration of dC^{PPI} derivatives (**1**−**3a**) and quenching efficiencies (F_q) of dC^{PPI} derivatives (X = **1**−**3a** and **4a**) in single or double-stranded oligonucleotides. ^{1}H NMR and ^{13}C NMR spectra of all the new products. This material is available free of charge via the Internet at http://pubs.acs.org.

References and Notes

(1) (a) Nordlund, T. M.; Andersson, S.; Nilsson, L.; Rigler, R.; Graeslund, A.; McLaughlin, L. W. *Biochemistry* **1989**, *28*, 9095–9103. (b) Frey, M. W.; Sowers, L. C.; Millar, D. P.; Benkovic, S. J. *Biochemistry* **1995**, *34*, 9185–92. (c) Roberts, R. J. *Cell* **1995**, *82*, 9–12. (d) Millar, D. P. *Curr. Opin. Struct. Biol.* **1996**, *6*, 322–326. (e) Stivers, J. T. *Nucleic Acids Res.* **1998**, *26*, 3837–3844. (f) Moser, A. M.; Patel, M.; Yoo, H.; Balis, F. M.; Hawkins, M. E. *Anal. Biochem.* **2000**, *281*, 216–222. (g) Deprez, E.; Tauc, P.; Leh, H.; Mouscadet, J. F.; Auclair, C.; Hawkins, M. E.; Brochon, J. C. *Proc. Natl. Acad. Sci. U.S.A.* **2001**, *98*, 10090–10095. (h) Wojtuszewski, K.; Hawkins, M. E.; Cole, J. L.; Mukerji, I. *Biochemistry* **2001**, *40*, 2588–2598. (i) Liu, C.; Martin, C. T. *J. Biol. Chem.* **2002**, *277*, 2725–2731. (j) Jiao, Y.; Stringfellow, S.; Yu, H. *J. Biomol. Struct. Dyn.* **2002**, *19*, 629–634. (k) Hariharan, C.; Reha-Krantz, L. J. *Biochemistry* **2005**, *44*, 15674–15684. (l) Hariharan, C.; Bloom, L. B.; Helquist, S. A.; Kool, E. T.; Reha-Krantz, L. J. *Biochemistry* **2006**, *45*, 2836–2844. (m) Andreatta, D.; Sen, S.; Pérez Lustres, J. L.; Kovalenko, S. A.; Ernsting, N. P.; Murphy, C. J.; Coleman, R. S.; Berg, M. A. *J. Am. Chem. Soc.* **2006**, *128*, 6885–6892. (n) Srivatsan, S. G.; Tor, Y. *J. Am. Chem. Soc.* **2007**, *129*, 2044–2053.

(2) (a) Ward, D. C.; Reigh, E.; Stryer, L. *J. Biol. Chem.* **1969**, *244*, 1228–37. (b) Sowers, L. C.; Fazakerley, G. V.; Erija, R.; Kaplan, B. E.; Goodman, M. F. *Proc. Natl. Acad. Sci. U.S.A.* **1986**, *83*, 5434–5438. (c) Rachofsky, E. L.; Seibert, E.; Stivers, J. T.; Osman, R.; Ross, J. B. A. *Biochemistry* **2001**, *40*, 957–967. (d) Christine, K. S.; MacFarlane, A. W., IV; Yang, K.; Stanley, R. J. *J. Biol. Chem.* **2002**, *277*, 38339–38344. (e)

Roy, S. *Methods Enzymol.* **2003**, *370*, 568–576. (f) Hoffman, P. D.; Wang, H.; Lawrence, C. W.; Iwai, S.; Hanaoka, F.; Hays, J. B. *DNA Repair* **2005**, *4*, 983–993.

(3) Ramreddy, T.; Kombrabail, M; Krishnamoorthy, G.; Rao, B. *J. Phys. Chem. B.* **2009**, *113*, 6840–6846.

(4) (a) Chabbert, M.; Lami, H.; Takahashi, M. *J. Biol. Chem.* **1991**, *266*, 5395–5400. (b) Li, Z.; Qian, X.; Xu, Y. *Dyes Pigments* **2002**, *54*, 247–252. (c) Seela, F.; Schweinberger, E.; Xu, K.; Sirivolu, V. R.; Rosemeyer, H.; Becker, E. *Tetrahedron* **2007**, *63*, 3471–3482.

(5) (a) Hawkins, M. E.; Pfleiderer, W.; Balis, F. M.; Porter, D.; Knutson, J. R. *Anal. Biochem.* **1997**, *244*, 86–95. (b) Hawkins, M. E.; Balis, F. M. *Nucleic Acids Res.* **2004**, *32*, e62.

(6) (a) Seibert, E.; Ross, J. B. A.; Osman, R. *J. Mol. Biol.* **2003**, *330*, 687–703. (b) Roca, A. I.; Singleton, S. F. *J. Am. Chem. Soc.* **2003**, *125*, 15366–15375. (c) Shchyolkina, A. K.; Kaluzhny, D. N.; Borisova, O. F.; Hawkins, M. E.; Jernigan, R. L.; Jovin, T. M.; Arndt-Jovin, D. J.; Zhurkin, V. B. *Nucleic Acids Res.* **2004**, *32*, 432–440.

(7) (a) Liu, C.; Martin, C. T. *J. Bio. Chem.* **2002**, *277*, 2725–2731. (b) Berry, D. A.; Jung, K.; Wise, D. S.; Sercel, A. D.; Pearson, W. H.; Mackie, H.; Randolph, J. B.; Somers, R. L. *Tetrahedron Lett.* **2004**, *45*, 2457–2461. (c) Dash, C.; Rausch, J. W.; Le Grice, S. F. J. *Nucleic Acids Res.* **2004**, *32*, 1539–1547. (d) Tinsley, R. A.; Walter, N. G. *RNA* **2006**, *12*, 522–529. (e) Marti, A. A.; Jockusch, S.; Li, Z.; Ju, J.; Turro, N. J. *Nucleic Acids Res.* **2006**, *34*, e50.

(8) (a) Srivatsan, S. G.; Tor, Y. *J. Am. Chem. Soc.* **2007**, *129*, 2044–2053. (b) Srivatsan, S. G.; Tor, Y. *Tetrahedron* **2007**, *63*, 3601–3607.

(9) (a) Okamoto, A.; Tainaka, K.; Saito, I. *J. Am. Chem. Soc.* **2003**, *125*, 4972–4973. (b) Okamoto, A.; Tainaka, K.; Saito, I. *Chem. Lett.* **2003**, *32*, 684–685. (c) Okamoto, A.; Tainaka, K.; Saito, I. *Photomed. Photobiol.* **2003**, *25*, 39–40.

(10) (a) Lin, K. Y.; Jones, R. J.; Matteucci, M. *J. Am. Chem. Soc.* **1995**, *117*, 3873–3874. (b) Eldrup, A. B.; Nielsen, B. B.; Haaima, G.; Rasmussen, H.; Kastrup, J. S.; Christensen, C.; Nielsen, P. E. *Eur. J. Org. Chem.* **2001**, *9*, 1781–1790. (c) Wilhelmsson, L. M.; Holmen, A.; Lincoln, P.; Nielsen, P. E.; Norden, B. *J. Am. Chem. Soc.* **2001**, *123*, 2434–2435. (d) , L. M.; Sandin, P.; Holmen, A.; Albinsson, B.; Lincoln, P.; Norden, B. *J. Phys. Chem. B.* **2003**, *107*, 9094–9101. (e) Engman, K. C.; Sandin, P.; Osborne, S.; Brown, T.; Billeter, M.; Lincoln, P.; Norden, B.; Albinsson, B.; Wilhelmsson, L. M. *Nucleic Acids Res.* **2004**, *32*, 5087–5095. (f) Sandin, P.; Wilhelmsson, L. M.; Lincoln, P.; Powers, V. E. C.; Brown, T.; Albinsson, B. *Nucleic Acids Res.* **2005**, *33*, 5019–5025.

(11) (a) Miyata, K.; Tamamushi, R.; Ohkubo, A.; Taguchi, H.; Seio, K.; Santa, T.; Sekine, M. *Org. Lett.* **2006**, *8*, 1545–1548. (b) Miyata, K.; Mineo, R.; Tamamushi, R.; Mizuta, M.; Ohkubo, A.; Taguchi, H.; Seio, K.; Santa, T.; Sekine, M. *J. Org. Chem.* **2007**, *72*, 102–108. (c) Mizuta, M.; Miyata, K.; Seio, K.; Sekine, M. *J. Org. Chem.* **2007**, *72*, 5046–5055. (d) Mizuta, M.; Seio, K.; Miyata, K.; Ohkubo, A.; Taguchi, H.; Sekine, M. *Nucleosides Nucleotides Nucleic Acids* **2007**, *26*, 1335–1338.

(12) (a) Sauer, M.; Han, K.-T.; Mueller, R.; Nord, S.; Schulz, A.; Seeger, S.; Wolfrum, J.; Arden-Jacob, J.; Deltau, G.; Marx, N. J.; Zander, C.; Drexhage, K. H. *J. Fluorescence* **1995**, *5*, 247–61. (b) Edman, L.; Mets, U.; Rigler, R. *Proc. Natl. Acad. Sci. U.S.A.* **1996**, *93*, 6710–6715. (c) Widengren, J.; Dapprich, J.; Rigler, R. *Chem. Phys.* **1997**, *216*, 417–426. (d) Nord, S.; Sauer, M.; Arden-Jacob, J.; Drexhage, K. H.; Lieberwirth, U.; Seeger, S.; Wolfrum, J. *J. Fluorescence* **1997**, *7*, 79S–81S. (e) Widengren, J.; Dapprich, J.; Rigler, R. *Chem. Phys.* **1997**, *216*, 417–426. (f) Eggeling, C.; Fries, J. R.; Brand, L.; Gunther, R.; Seidel, C. A. M. *Proc. Natl. Acad. Sci. U.S.A.* **1998**, *95*, 1556–1561.

(13) (a) Sauer, M.; Drexhage, K. H.; Lieberwirth, U.; Muller, R.; Nord, S.; Zander, C. *Chem. Phys. Lett.* **1998**, *284*, 153–163.

(14) (a) Lewis, F. D.; Wu, T.; Zhang, Y.; Letsinger, R. L.; Greenfield, S. R.; Wasielewski, M. R. *Science* **1997**, *277*, 673–676. (b) Lewis, F. D.; Wu, T.; Liu, X.; Letsinger, R. L.; Greenfield, S. R.; Miller, S. E.; Wasielewski, M. R. *J. Am. Chem. Soc.* **2000**, *122*, 2889–2902. (c) Lewis, F. D.; Liu, X.; Liu, J.; Miller, S. E.; Hayes, R. T.; Wasielewski, M. R. *Nature* **2000**, *406*, 51–53. (d) Lewis, F. D.; Letsinger, R. L.; Wasielewski, M. R. *Acc. Chem. Res.* **2001**, *34*, 159–170.

(15) (a) Rehm, D.; Weller, A. *Isr. J. Chem.* **1970**, *8*, 259–71. (b) Marcus, R. A.; Sutin, N. *Biochim. Biophys. Acta, Rev. Bioenerg.* **1985**, *811*, 265–322.

(16) (a) Lakowicz, J. R. *Principles of Fluorescence Spectroscopy*, 2nd ed.; Kluwer Academic: New York, 1999.

(17) Weller, A. *Z. Phys. Chem.* **1982**, *133*, 93–8.

(18) Steenken, S.; Jovanovic, S. V. *J. Am. Chem. Soc.* **1997**, *119*, 617–618.

(19) Adams, M. J.; Highfield, J. G.; Kirkbright, G. F. *Anal. Chem.* **1977**, *49*, 1850–1852.

(20) Cornell, W. D.; Cieplak, P.; Bayly, C. I.; Gould, I. R.; Merz, K. M., Jr.; Ferguson, D. M.; Spellmeyer, D. C.; Fox, T.; Caldwell, J. W.; Kollman, P. A. *J. Am. Chem. Soc.* **1995**, *117*, 5179–97.

(21) Frisch, M. J.; Trucks, G. W.; Schlegel, H. B.; Scuseria, G. E.; Robb, M. A.; Cheeseman, J. R.; Montgomery, J. A., Jr.; Vreven, T.; Kudin, K. N.; Burant, J. C.; Millam, J. M.; Iyengar, S. S.; Tomasi, J.; Barone, V.; Mennucci, B.; Cossi, M.; Scalmani, G.; Rega, N.; Petersson, G. A.; Nakatsuji, H.; Hada, M.; Ehara, M.; Toyota, K.; Fukuda, R.; Hasegawa, J.; Ishida, M.; Nakajima, T.; Honda, Y.; Kitao, O.; Nakai, H.; Klene, M.; Li, X.; Knox, J. E.; Hratchian, H. P.; Cross, J. B.; Bakken, V.; Adamo, C.; Jaramillo, J.; Gomperts, R.; Stratmann, R. E.; Yazyev, O.; Austin, A. J.; Cammi, R.; Pomelli, C.; Ochterski, J. W.; Ayala, P. Y.; Morokuma, K.; Voth, G. A.; Salvador, P.; Dannenberg, J. J.; Zakrzewski, V. G.; Dapprich, S.; Daniels, A. D.; Strain, M. C.; Farkas, O.; Malick, D. K.; Rabuck, A. D.; Raghavachari, K.; Foresman, J. B.; Ortiz, J. V.; Cui, Q.; Baboul, A. G.; Clifford, S.; Cioslowski, J.; Stefanov, B. B.; Liu, G.; Liashenko, A.; Piskorz, P.; Komaromi, I.; Martin, R. L.; Fox, D. J.; Keith, T.; Al-Laham, M. A.; Peng, C. Y.; Nanayakkara, A.; Challacombe, M.; Gill, P. M. W.; Johnson, B.; Chen, W.; Wong, M. W.; Gonzalez, C.; Pople, J. A. *Gaussian 03, revision C.02*; Gaussian, Inc.: Wallingford, CT, 2004.

JP807562C